Supporting Information

Pushing the Limits of Oxygen Balance in Pentazolate Salts via the Theoretical Construction of Oxidizer-based Cocrystal

Zhenyu Yuan [a], *Chen Yang* [a]*, *Lei Wang* [a] *Changlin Zhou* [a]*

[a] College of Materials and Chemical Engineering, Key Laboratory of Inorganic Nonmetallic Crystalline and Energy Conversion Materials, China Three Gorges University, China.

* Corresponding authors. Email address: yangchen@ctgu.edu.cn (Chen Yang); clzhou@ctgu.edu.cn (Changlin Zhou)

Table of contents

SI 1. Reported *c*-N_5^- cocrystals.

Table S1. Selected parameters of reported *c*-N_5^- cocrystals.

Crystal	Space Group	Formula Unit	*d* (g cm^{-3})	OB%	Ref
$[NH_4][N_5]\cdot 1/2H_2O$ (a)	14	4	1.509	-22.86%	[1]
$([NH_3OH][N_5])_2\cdot[NH_3OH]Cl\cdot H_2O$(b)	14	4	1.588	-16.24%	[2]
[HTATOT][N_5]·TATOT (c)	14	4	1.664	-52.77%	[3]
$[NH_4][N_5]\cdot 1/6[NH_4]Cl$ (d)	227	2	1.438	-38.52%	[4]
$2[N_2H_5][N_5]\cdot$PDO (e)	2	1	1.608	-45.28%	[5]
[HTATOT][N_5]·Ma (f)	15	8	1.743	-56.98%	[6]
[HDNAZ][N_5]·DNAZ (g)	56	4	1.679	-15.34%	[7]
$[NH_3OH][N_5]$/18C6 (h)	19	4	1.292	-82.61%	[8]
[TNHAHP][N_5]·[TNHAHP][NO_3](i)	61	8	1.687	-22.92%	[9]
$[NH_4][N_5]\cdot$DAF (j)	19	4	1.569	-42.55%	[10]
$[N_2H_5][N_5]\cdot$DAF (k)	14	4	1.589	-43.35%	[10]
$[NH_3OH][N_5]\cdot$DAF (l)	15	8	1.604	-31.37%	[10]

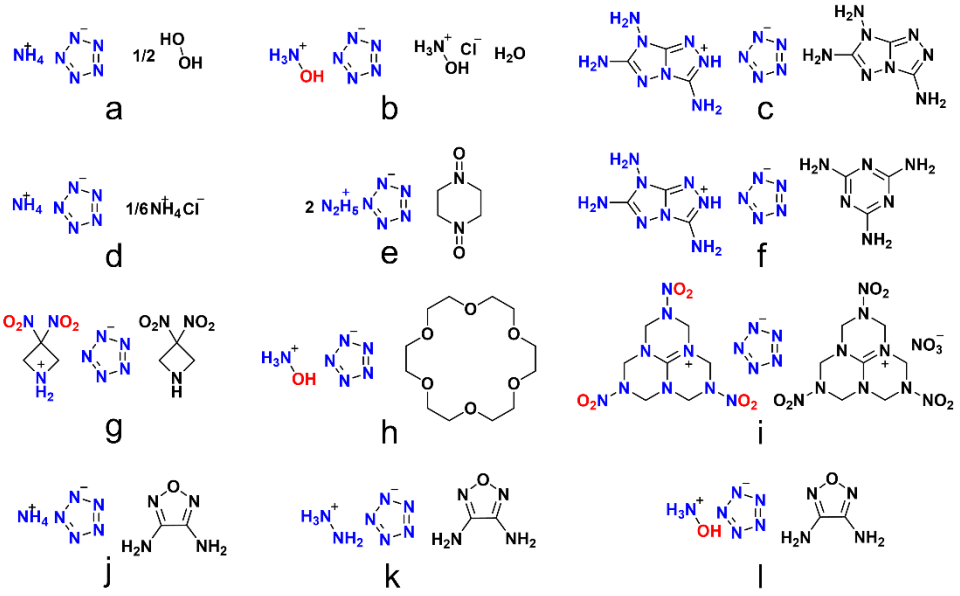

SI 2. Computational methods

Table S2. The energy and force convergence criteria.

Energy and force	maximum
geometry change	3×10^{-3} bohr
force component	4.5×10^{-4} hartree bohr^{-1}
root-mean-square geometry change	1.5×10^{-3} bohr
root-mean-square force	3×10^{-4} hartree bohr^{-1}

Table S3. Comparison of calculated and experimental crystal parameters for selected *c*-N_5^- cocrystals.

Crystal		*a* (Å)	*b* (Å)	*c* (Å)	*α* (°)	*β* (°)	*γ* (°)
$[NH_4][N_5]\cdot 1/2H_2O$	Experiment	3.84	13.19	9.19	90.00	96.73	90.00
	Calculation	3.56	12.59	8.46	90.00	97.69	90.00
	deviation (%)	7.23	4.58	-7.93	0.00	0.99	0.00
$2[N_2H_5][N_5]\cdot PDO$	Experiment	6.18	7.36	7.25	108.08	91.51	114.82
	Calculation	6.63	7.83	7.94	117.14	93.12	111.674
	deviation (%)	6.75	6.05	8.74	7.73	1.74	2.82
$[THZAP][N_5]\cdot[THZAP][NO_3]$	Experiment	11.92	16.29	30.18	90.00	90.00	90.00
	Calculation	11.19	15.77	28.61	90.00	90.00	90.00
	deviation (%)	6.08	3.16	5.20	0.00	0.00	0.00
$[NH_4][N_5]\cdot DAF$	Experiment	3.71	10.04	21.37	90.00	90.00	90.00

Calculation	3.57	9.33	19.97	90.00	90.00	90.00
deviation (%)	3.92	7.11	6.56	0.00	0.00	0.00

Table S4. A comparison of the lattice parameters of $2[N_2H_5][N_5]\cdot$PDO obtained from simulation and experimental measurements.

	a (Å)	*b* (Å)	*c* (Å)	*d* (g cm^{-3})	V (Å^3)
Experiment	6.630	7.834	7.945	1.608	328.63
Simulation	6.051	7.507	7.534	1.684	313.87
Relative deviation (%)	3.95	3.82	5.51	4.73	4.41

SI 3. Crystal structures

Table S5 Relative energies for the ranked $[NH_4][N_5]\cdot$ADN structures.

$[NH_4][N_5]\cdot$ADN						
Space group	PBE-D3(BJ)		PBE0-D3(BJ)		RPBE-D3(BJ)	
	Rank	ΔE^a	Rank	ΔE^b	Rank	ΔE^c
$P2_1/c$, Z=4	7	13.50	5	6.25	1	0
$P2_1/c$, Z=4	1	0	1	0	2	15.08
$P2_1/c$, Z=4	2	2.47	2	1.37	3	19.44
Pbca, Z=8	3	5.96	4	4.06	4	39.61
$Pna2_1$, Z=4	4	6.35	3	3.76	5	44.89
$P2_1/c$, Z=4	6	10.84	7	10.43	6	56.23
$P2_12_12_1$, Z=4	5	9.64	6	7.52	7	69.61
$P1$, Z=4	8	33.65	8	33.19	8	118.5

(a) PBE-D3(BJ), (b) PBE0-D3(BJ) and (c) RPBE-D3(BJ) functionals were employed with the TZV2P-MOLOPT-GTH basis set to calculate the total energies per asymmetric unit (in kJ/mol) relative to the most stable structure.

Table S6 Relative energies for the ranked $[N_2H_5][N_5]$·HNF structures.

$[N_2H_5][N_5]$·HNF						
Space group	PBE-D3(BJ)		PBE0-D3(BJ)		RPBE-D3(BJ)	
	Rank	ΔE^a	Rank	ΔE^b	Rank	ΔE^c
Pna2$_1$, *Z*=4	1	0	2	8.586	1	0
Pna2$_1$, *Z*=4	2	0.107	1	0	2	1.76
P2$_1$/c, *Z*=4	7	25.333	7	30.63	3	19.26
Pbca, *Z*=8	4	17.30	5	20.75	4	34.15
P2$_1$*2*$_1$*2*$_1$, *Z*=4	5	20.31	8	44.42	5	44.13
*P*1, *Z*=4	3	10.36	3	10.33	6	46.00
Pna2$_1$, *Z*=4	6	20.98	4	20.57	7	73.45
Pna2$_1$, *Z*=4	8	25.53	6	29.74	8	101.48

(a) PBE-D3(BJ), (b) PBE0-D3(BJ) and (c) RPBE-D3(BJ) functionals were employed with the TZV2P-MOLOPT-GTH basis set to calculate the total energies per asymmetric unit (in kJ/mol) relative to the most stable structure.

Table S7. A comparison of the lattice parameters of $2[N_2H_5][N_5]$·PDO obtained from simulation and experimental measurements.

	*P*1	*P*-1
Lattice energy (kJ mol^{-1})	-416.612	-425.427

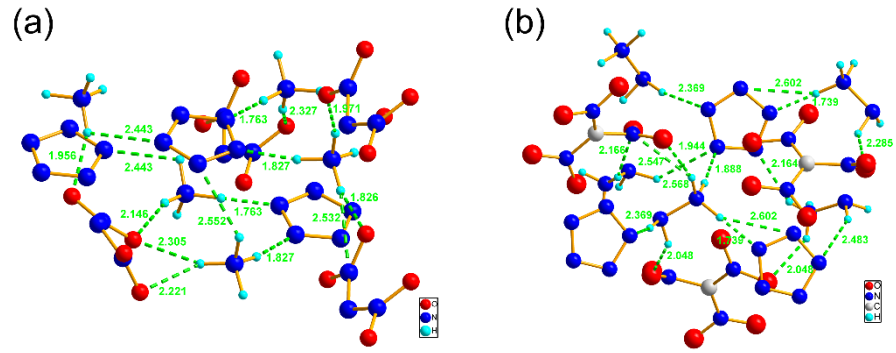

Fig. S1 hydrogen-bond distributions(a) $[NH_4][N_5]\cdot$ADN and (b) $[N_2H_5][N_5]\cdot$HNF.

Table S8 Hydrogen bonds for $[NH_4][N_5]\cdot$ADN.

D-H...A	D-H (Å)	H...A (Å)	D...A (Å)	D-H...A (°)
N6-H6A...O4	1.04	2.15	3.1540	163
N6-H6B...O3	1.04	1.96	2.9460	157
N6-H6B...N4	1.04	2.45	2.9850	111
N6-H6C...N5	1.04	2.58	3.0302	106
N6-H6C...O4	1.04	2.33	3.2991	156
N6-H6D...N1	1.07	1.72	2.7904	179
N7-H7A...N3	1.04	2.53	3.0354	109
N7-H7A...O1	1.04	1.97	2.9791	162
N7-H7B...O2	1.05	1.83	2.8495	163
N7-H7B...N10	1.05	2.51	3.5706	169
N7-H7C...O2	1.03	2.22	2.9821	129
N7-H7C...O4	1.03	2.30	3.290	159
N7-H7C...N2	1.06	1.83	2.8890	171

Table S9 Hydrogen bonds for $[N_2H_5][N_5]\cdot$HNF.

D-H...A	D-H (Å)	H...A (Å)	D...A (Å)	D-H...A (°)
N1-H1A...N5	1.03	2.37	3.3828	168
N1-H1B...O4	1.03	2.41	3.0217	117

N1-H1B...O6	1.03	2.29	3.1209	137
N2-H2A...N8	1.07	1.74	2.7959	170
N2-H2A...N9	1.07	2.60	3.5524	148
N2-H2B...O3	1.04	2.40	2.8145	103
N2-H2B...O6	1.04	1.94	2.9256	157
N2-H2B...N10	1.04	2.55	3.2915	128
N2-H2C...N6	1.05	1.89	2.9230	169
N3-H3A...N7	1.05	1.90	2.9421	171
N3-H3B...N1	1.05	1.99	3.0038	160
N3-H3B...O1	1.05	2.48	2.8728	101
N3-H3B...O5	1.05	2.44	2.9443	108
N3-H3C...O3	1.05	1.81	2.8099	159
N3-H3C...N12	1.05	2.43	3.2490	134
N4-H4A...N5	1.03	2.48	3.4164	151
N4-H4B...N6	1.03	2.57	3.3825	136

SI 5. Structural stability

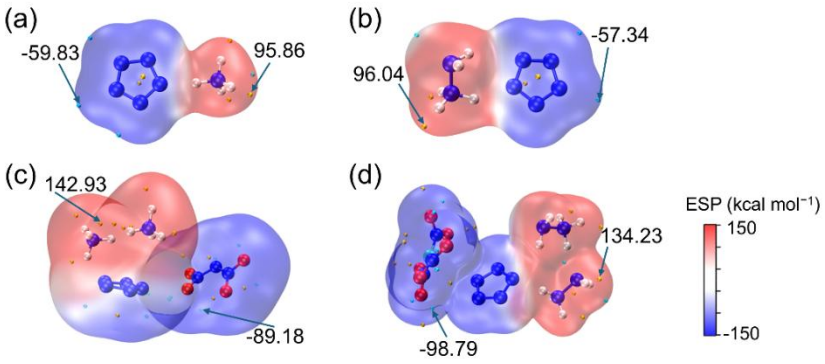

Fig. S2 ESP-mapped surfaces of $[NH_4][N_5]$ (a), $[N_2H_5][N_5]$ (b), $[NH_4][N_5]\cdot$ADN (c) and $[N_2H_5][N_5]\cdot$HNF (d)

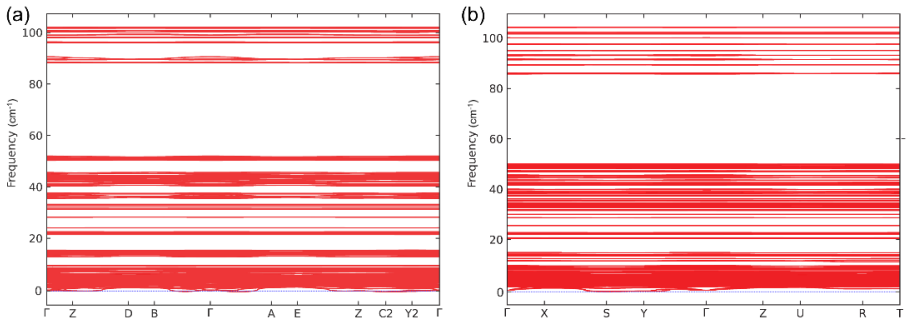

Fig. S3 Phonon spectrum of $[NH_4][N_5]\cdot$ADN (a) and $[N_2H_5][N_5]\cdot$HNF (b)

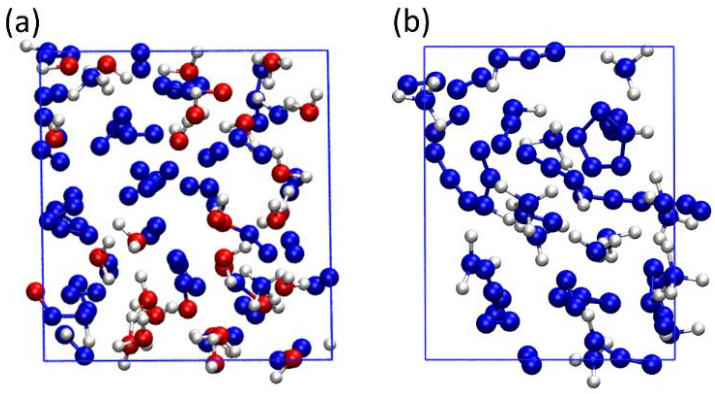

Fig. S4 Simulation snapshots of (a) $[NH_4][N_5]\cdot$ADN and (b) $[NH_4][N_5]$ at 1800 K after 25 ps.

Table S10. Number of major species from the decomposition of $[NH_4][N_5]\cdot$ADN and $[NH_4][N_5]$ at 1800 K.

	N_5	HN_5	N_2	HN_3	N_3^-	NH_3	H_2O	N_2O
$[NH_4][N_5]\cdot$ADN	0	0	27	1	0	1	15	2
$[NH_4][N_5]$	1	2	8	6	2	5	0	0

SI 6. Heat of formation.

The solid-state heat of formation (cocrystal ΔH_f) was calculated based on a Born–Haber energy cycle[11] with the following simplified equation for calculation:

ΔH_f (cocrystal, 298K) =2ΔH_f (cation , 298K) + ΔH_f (anion 1, 298K) + ΔH_f (anion 2, 298K) – ΔHsub

The heat of sublimation can be estimated using the DFT method with the RPBE (revised Perdew Burke-Ernzerhof) exchange-correlation functional in CP2K program with the TZV2P-MOLOPT-GTH basis set.

Table S11. The related heat of formations for several species.

	Heat of formation (kJ mol^{-1} 298K)
NH_4 cation [a]	639.2
DN anion [b]	-156.2
N_2H_5 cation [a]	776.1
NF anion [c]	-228.8
N_5 anion [a]	258.7
$[NH_4][N_5]$·ADN	644.2
$[N_2H_5][N_5]$·HNF	860.1

[a] Ref 12. [b] Ref 13. [c] Ref 11.

SI 7. Detonation performance

Detonation velocity (D in km s^{-1}) and detonation pressure (P in GPa) were predicted by the empirical Kamlet–Jacobs[14] as follows:

$$D = 1.01\left(N\bar{M}^{\frac{1}{2}}Q^{\frac{1}{2}}\right)^{\frac{1}{2}}(1 + 1.30\rho) \quad (3)$$

$$P = 1.558\rho^2 N\bar{M}^{\frac{1}{2}}Q^{\frac{1}{2}} \quad (4)$$

in which N (mol g^{-1}) is the moles of detonation gases per gram explosive, M (g mol^{-1}) represents the average molecular weight of these gases, and Q (cal g^{-1}) is the heat of detonation.

Table S12. Formulas of N, $\bar{M}$, and Q for $C_aH_bO_cN_d$ Explosives

	$c \geq 2a + \frac{b}{2}$	$2a + \frac{b}{2} > c > \frac{b}{2}$	$\frac{b}{2} > c$
N	$\frac{b + c + 2d}{4M}$	$\frac{b + c + 2d}{4M}$	$\frac{b + d}{2M}$
$\bar{M}$	$\frac{4M}{b + c + 2d}$	$\frac{56d + 88c - 8b}{b + 2c + 2d}$	$\frac{2b + 28d + 32c}{b + d}$
Q	$\frac{28.9b + 94.05c + 0.239\Delta H_f}{4M}$	$\frac{5.3875b + 47.025c + 0.239\Delta H_f}{4M}$	$\frac{57.8c + 0.239\Delta H_f}{4M}$

SI 8. References

1. J. Luo, H. Xia, W. Zhang, S. Song, Q. Zhang, *J. Mater. Chem. A*, 2020, **8**, 12334-12338.

2. Y. Yuan, T. Hou, D. Li, Y. Xu, M. Lu, *Chin. J. Energy Mater.*, 2022, **30**, 96-102.

3. C. Yang, L. Chen, W. Wu, C. Zhang, C. Sun, Y. Du, B. Hu, *ACS Appl. Energy Mater.*, 2021, **4**, 146-153.

4. Y. Xu, D. Li, P. Wang, Q. Lin, L. Ding, T. Hou, Y. Yuan, M. Lu, *J. Energetic Mater.*, 2023, **41**, 99-116.

5. J. Zhou, X. Li, T. Hou, Z. Xu, P. Wang, M. Lu, Y. Xu, *CrystEngComm*, 2023, **25**, 2027-2031.

6. Y. Xu, J. Zhou, X. Li, T. Hou, Z. Xu, P. Wang, M. Lu, *Commun. Mater.*, 2024, **5**, 25.

7. C. Yang, L. Chen, S. Chen, W. Wu, W. Yuan, J. Yao, C. Zhang, C. Sun, Y. Du, B. Hu, *Cryst. Growth Des.*, 2021, **21**, 4329-4336.

8. Chen, Z. Shen, D. Kong, C. Zhang, B. Hu, C. Gao, *CrystEngComm*, 2025,**27**, 5312-5318.

9. J. Zou, L. Zhang, Z. Chen, H. Li, Q. Zhou, X. Wang, M. Huang, S. Yu, H. Yang, *New J. Chem.*, 2025,**49**, 10922-10927

10. Chen, P. Gao, Z. Jin, Z. Shen, J. Sun, K. Deng, C. Zhu, B. Hu, C. Zhang, *Cryst. Growth Des.*, 2025, **25**, 6248-6257.

11. J. Zhang, Y. Feng, R. J. Staples, J. Zhang, J. M. Shreeve, *Nat. Commun.*, 2021, **12**, 2149**.**

12. K. O. Christe, D. A. Dixon, M. Vasiliu, R. Haiges, B. Hu, *Propellants, Explos., Pyrotech.*, 2019, **44**, 263-266.

13. H. Gao, C. Ye, C. M. Piekarski, J. M. Shreeve,*J. Phys. Chem. C*, 2007, **111**, 10718–10731.

14. J. Kamlet, S. J. Jacobs, *J. Chem. Phys.*, 1968, **48**, 23-35.